AD-A134 517 EXPERIMENTAL APPARATUS FOR STUDYING MOVING THERMOACOUSTIC SOURCES(U) TEXAS UNIV AT AUSTIN APPLIED RESEARCH LABS C R CULBERTSON ET AL. 15 JUL 83 1/1

UNCLASSIFIED ARL-TR-83-24 N00014-82-K-0425 F/G 9/5 NL

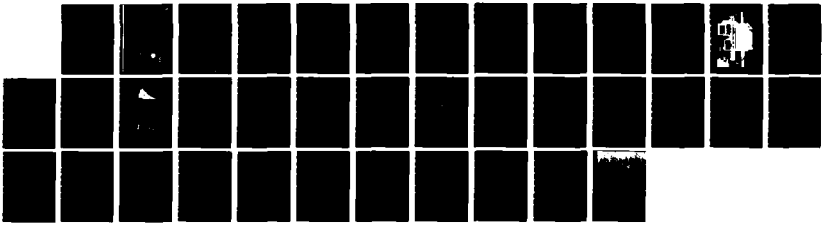

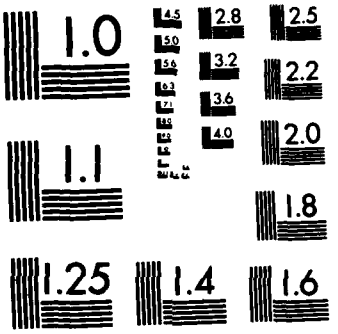

12

ARL-TR-83-24

Copy No. 3

AD-A136 [illegible]

EXPERIMENTAL APPARATUS FOR STUDYING MOVING THERMOACOUSTIC SOURCES

C. Robert Culbertson
Nicholas P. Chotiros
Yves H. Berthelot

APPLIED RESEARCH LABORATORIES
THE UNIVERSITY OF TEXAS AT AUSTIN
POST OFFICE BOX 8029, AUSTIN, TEXAS 78712-8029

15 July 1983

Technical Report

Prepared for:

OFFICE OF NAVAL RESEARCH
DEPARTMENT OF THE NAVY
ARLINGTON, VA 22217

REPORT DOCUMENTATION PAGE

READ INSTRUCTIONS BEFORE COMPLETING FORM

1. REPORT NUMBER	2. GOVT ACCESSION NO. AD-A134517
3. RECIPIENT'S CATALOG NUMBER	
4. TITLE (and Subtitle) EXPERIMENTAL APPARATUS FOR STUDYING MOVING THERMOACOUSTIC SOURCES	5. TYPE OF REPORT & PERIOD COVERED technical report
	6. PERFORMING ORG. REPORT NUMBER ARL-TR-83-24
7. AUTHOR(s) C. Robert Culbertson, Nicholas P. Chotiros, Yves H. Berthelot	8. CONTRACT OR GRANT NUMBER(s) N00014-82-K-0425
9. PERFORMING ORGANIZATION NAME AND ADDRESS Applied Research Laboratories, The University of Texas at Austin, Austin, TX 78712-8029	10. PROGRAM ELEMENT, PROJECT, TASK AREA & WORK UNIT NUMBERS
11. CONTROLLING OFFICE NAME AND ADDRESS Office of Naval Research, Department of the Navy, Arlington, VA 22217	12. REPORT DATE 15 July 1983
	13. NUMBER OF PAGES 32
14. MONITORING AGENCY NAME & ADDRESS(if different from Controlling Office)	15. SECURITY CLASS. (of this report) UNCLASSIFIED
	15a. DECLASSIFICATION/DOWNGRADING SCHEDULE

16. DISTRIBUTION STATEMENT (of this Report)

Approved for public release; distribution unlimited.

17. DISTRIBUTION STATEMENT (of the abstract entered in Block 20, if different from Report)

18. SUPPLEMENTARY NOTES

19. KEY WORDS (Continue on reverse side if necessary and identify by block number)

thermoacoustics
modulated laser
directivity

20. ABSTRACT (Continue on reverse side if necessary and identify by block number)

Sound is generated thermoacoustically when a modulated laser beam illuminates a volume of water. This report describes an experimental system developed to study the effects of moving the thermoacoustic source through the water. Motion of the source produces a direction dependent Doppler shift and, in some cases, an increase in the efficiency of the thermoacoustic process.

TABLE OF CONTENTS

LIST OF FIGURES

LIST OF TABLES

I. INTRODUCTION

The generation of directive sound by thermoacoustic sources has been studied theoretically and experimentally by both American[1-4] and Soviet[5-10] scientists. The thermoacoustic sound generation process involves heating and subsequent expansion of a region of fluid due to absorption of optical radiation. If the optical intensity is modulated, the illuminated region expands and contracts in sympathy with the modulation, thus producing sound. The directivity of thermoacoustically generated sound depends upon the optical absorption coefficient α of the medium, the acoustic wave number λ, and the radius a of the light beam. Three configurations of thermoacoustic source are shown in Fig. 1. A point source is produced if the beam radius and absorption length α^{-1} is small compared to the acoustic wavelength, as shown in Fig. 1(a). A disk source and rod source may also be realized, as shown in Figs. 1(b) and 1(c) respectively. For the rod source, a highly directive sound beam can be generated if a laser beam with small optical absorption, such as a blue-green laser, is used to illuminate the medium. Furthermore, the optical intensity decays exponentially due to absorption, so the amplitude of the rod source is shaded and minor lobes in the sound beam are thereby suppressed.

The Soviets have recently devoted considerable effort to the study of moving thermoacoustic sources. They cite[5,6] several benefits obtained by moving the source: increased efficiency, lengthened nearfield, and modification of directivity and sound frequency. Since drag and flow noise impose no limitations on moving a thermoacoustic source through water, even supersonic source speeds have been obtained.[5] There is a need to investigate the characteristics of moving thermoacoustic sources so that their usefulness in sonar applications can be evaluated. The Soviet research should be carefully reviewed and their experimental work extended to lower frequencies.

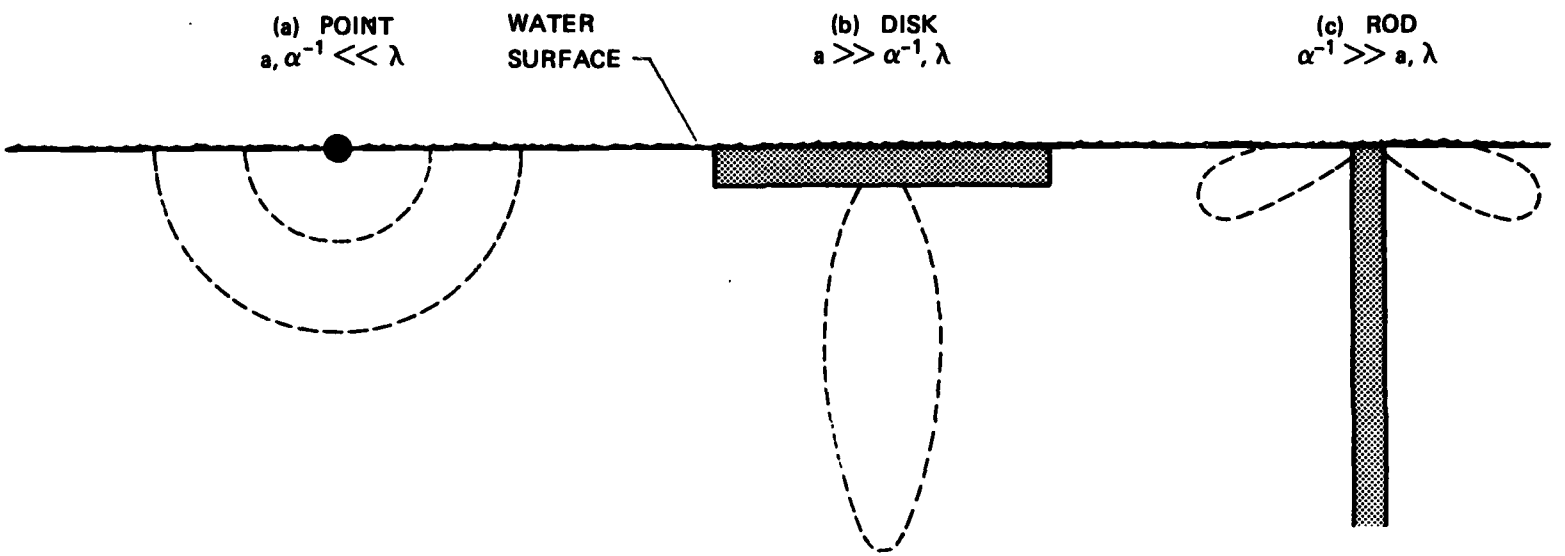

FIGURE 1
THERMOACOUSTIC SOURCE CONFIGURATIONS

ARL:UT
AS-81-1448
CRC-GA
11-20-81

Applied Research Laboratories, The University of Texas at Austin (ARL:UT), is developing an experimental system for the study of moving thermoacoustic sources. This report describes early development of the experimental apparatus and discusses the results of preliminary measurements made with the apparatus. A set of predictions for acoustic parameters associated with the apparatus is also presented. The work described in this report was conducted May - September 1982. Further development of the apparatus and experimental results will be described in a later report.

II. EXPERIMENTAL APPARATUS

The apparatus used to investigate moving thermoacoustic sources consists of a high power modulated laser, a means of deflecting the laser beam, and some acoustic receiving and signal processing hardware. A block diagram of the experimental system is shown in Fig. 2. A laser with interchangeable (neodymium) Nd:glass and ruby rods produces a 1 msec pulse that is intensity modulated at a frequency between 5 kHz and 80 kHz. The laser beam is directed to a rotating mirror, the speed of which is controlled by a synchronous motor with a variable frequency power supply. The mirror deflects the laser beam so that the thermoacoustic source moves through the water.

A description of each component of the experimental system is given below.

A. Laser

The laser was procured under a previous ONR contract (Contract N00014-70-A-0166, Task 0015) for work related to stationary thermoacoustic arrays. A picture of the laser and a diagram of its optical train configuration are shown in Figs. 3 and 4, respectively. The laser head assembly contains a flashlamp for optical pumping of the lasing element, which can be either a ruby or Nd:glass rod. A Brewster stack is used to polarize the output of the Nd:glass rod, and a calcite prism polarizer is used with the ruby rod. A 100% back mirror and an output mirror complete the optical cavity.

The intensity of the light produced by this cavity is modulated by the Pockels cell and prism analyzer. Figure 5 illustrates the principle of laser beam modulation. The Pockels cell consists of an electrically driven KD*P crystal immersed in a protective dielectric fluid. When

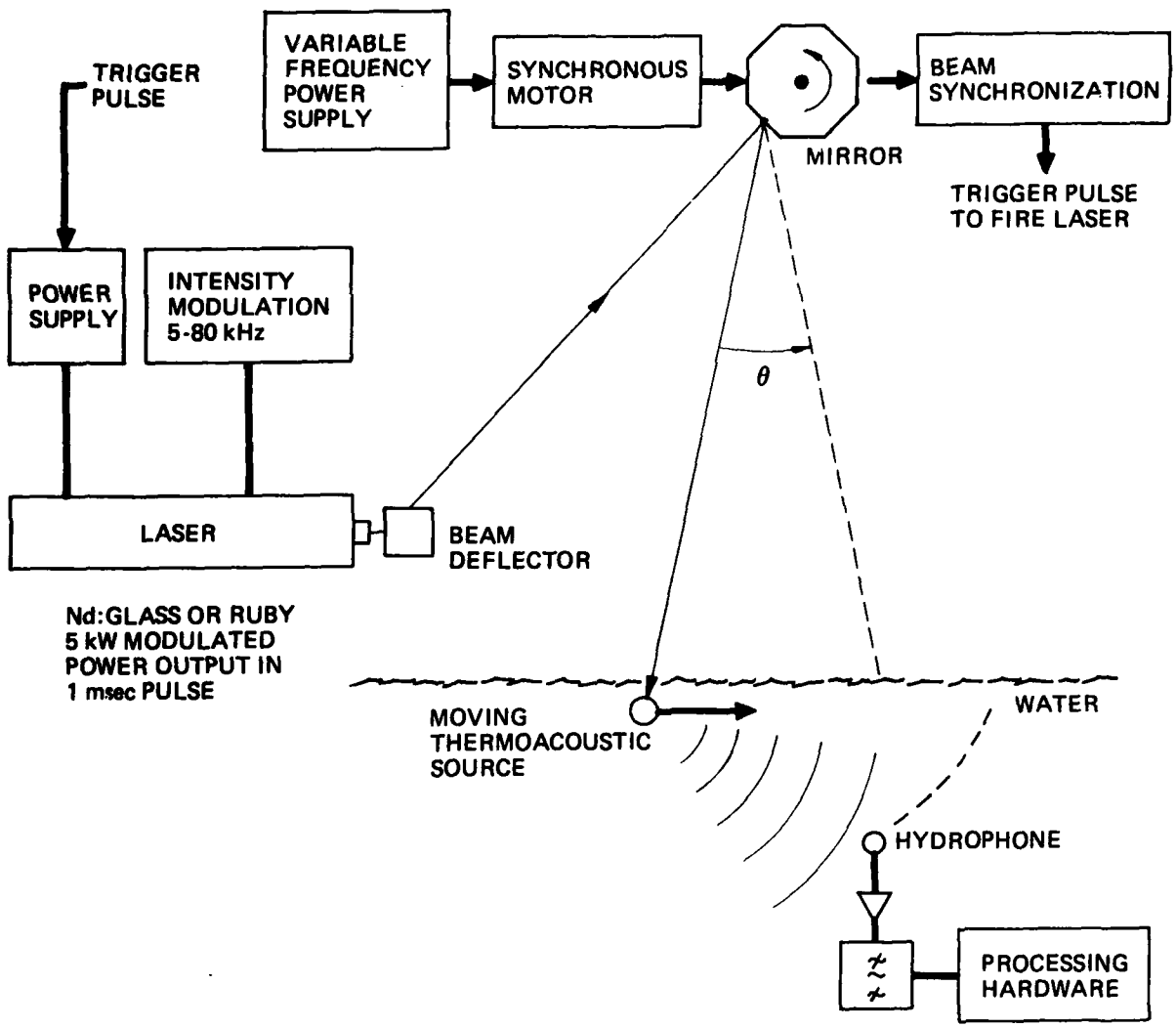

FIGURE 2
BLOCK DIAGRAM OF EXPERIMENTAL SYSTEM

ARL:UT
AS-81-1449
CRC - GA
11-20-81

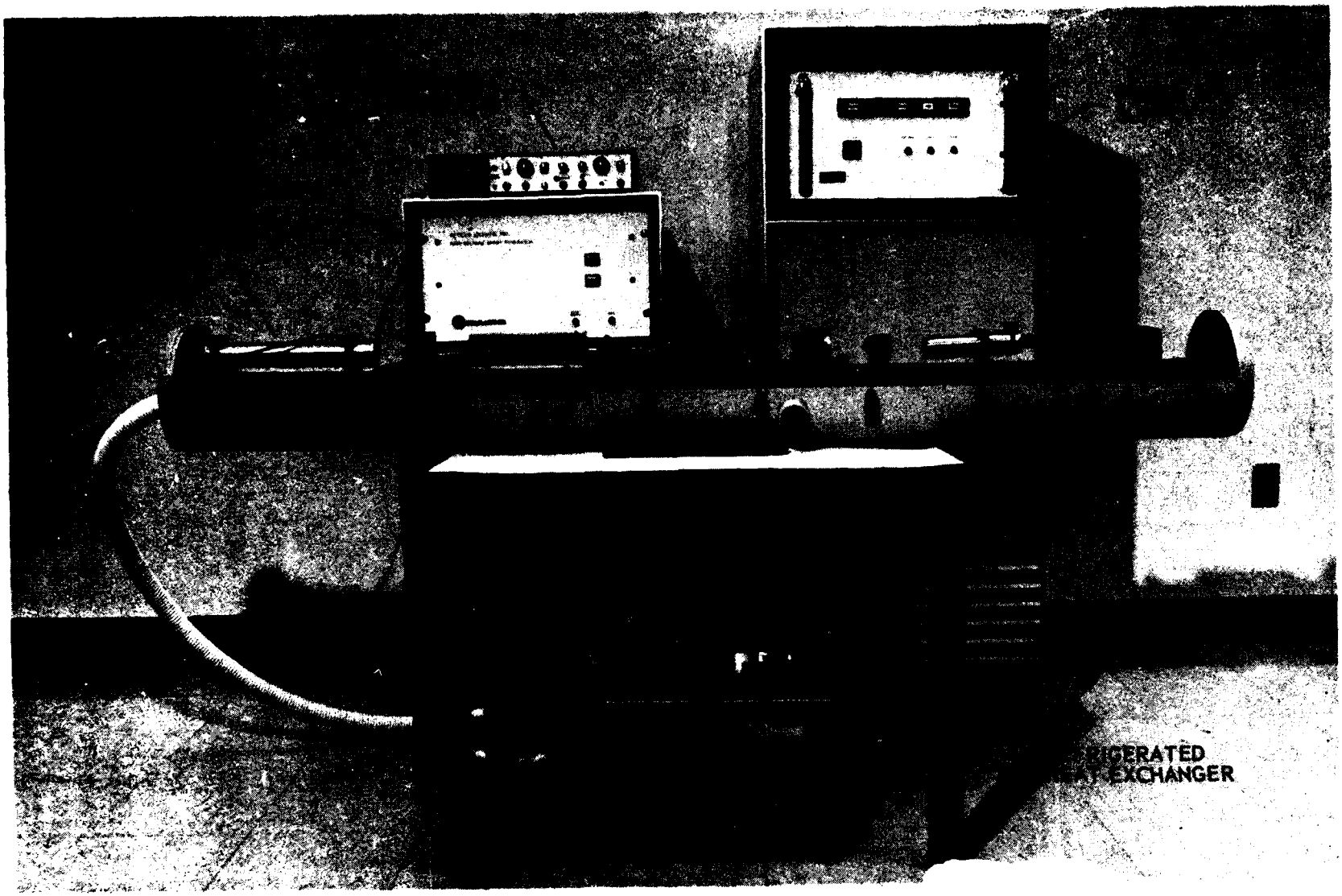

FIGURE 3
MODULATED LASER SYSTEM

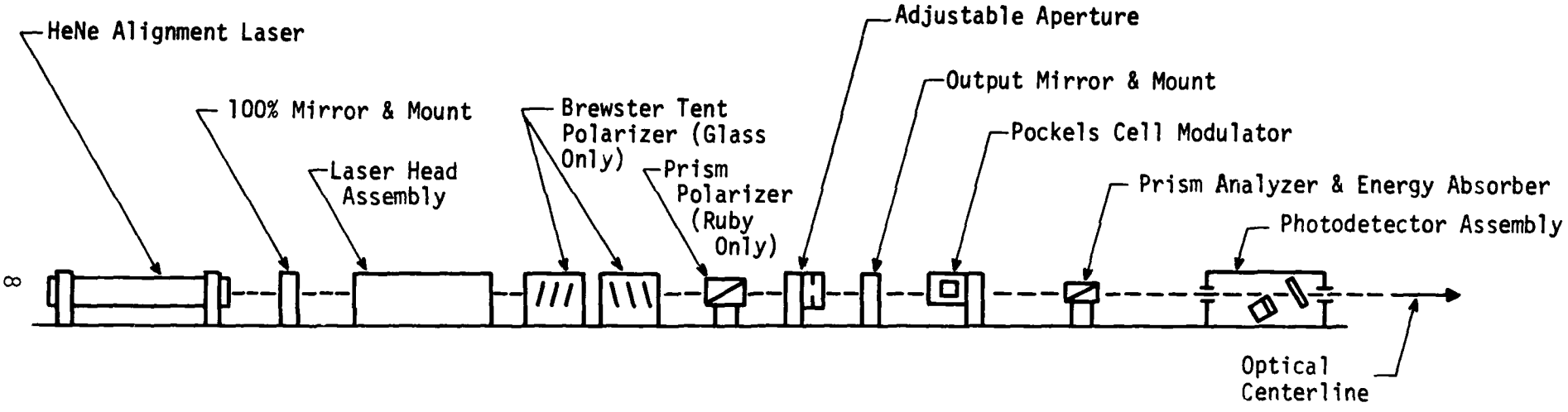

FIGURE 4

OPTICAL TRAIN CONFIGURATION

AS-75-1616
CRC-0207-2

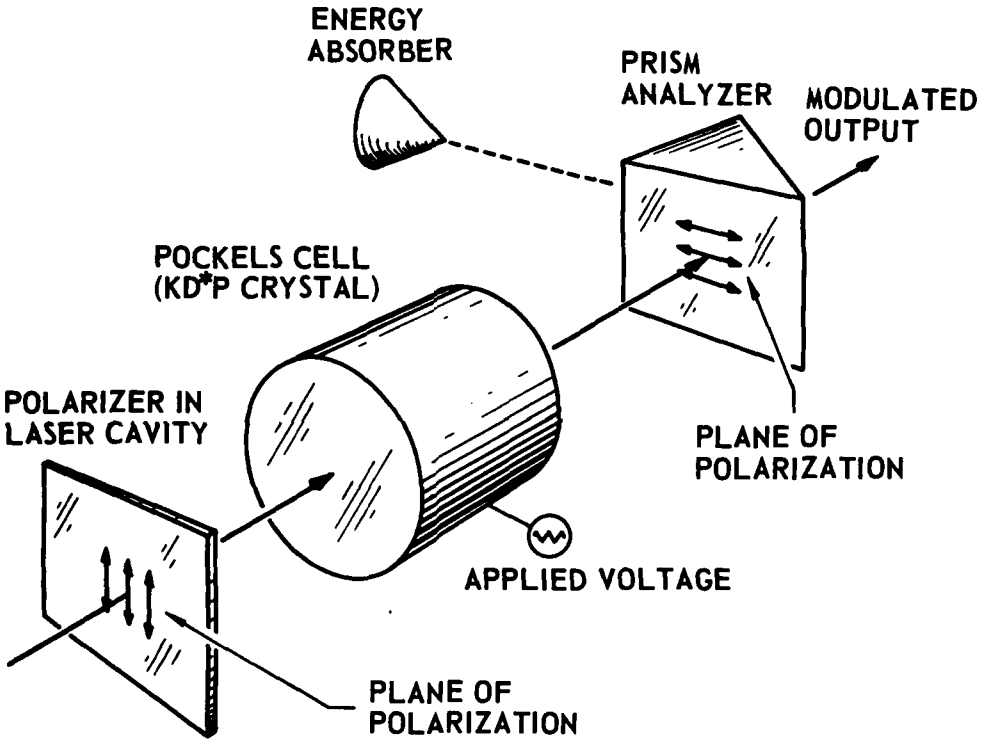

FIGURE 5
LASER BEAM MODULATION

ARL - UT
AS-75-513
CRC - RFO
4 - 10 - 75

voltage is applied to the electrodes of the KD*P crystal, the Pockels cell rotates the plane of polarization of light passing through it. The amount of rotation is nonlinearly related to the applied voltage. As shown in Fig. 5, the prism analyzer is a polarizer with its polarization plane perpendicular to that of the polarizer in the laser cavity. With no voltage applied to the Pockels cell, there is no transmission of the laser beam through the prism analyzer. When the half-wave voltage is applied to the Pockels cell, the plane of polarization of light incident on the analyzer is rotated 90^{o}, and all of the beam is transmitted through the system.

The transmittance of the modulation system is given by

$$I = I_o \sin^2 \frac{\pi V}{2V_{1/2}} \quad , \tag{1}$$

where

I = transmitted light intensity,
I_o = incident light intensity,
V = voltage applied to Pockels cell, and
$V_{1/2}$ = half-wave voltage of the KD*P crystal.

By driving the Pockels cell with a triangular wave voltage of amplitude $V_{1/2}\omega t/\pi$, it is possible to effect a sine-squared modulation of the form

$$\begin{aligned} I &= I_o \sin^2\left(\frac{1}{2}\omega t\right) \\ &= I_o\left(\frac{1}{2} - \frac{1}{2}\cos\omega t\right) \end{aligned} \tag{2}$$

This modulation is illustrated in Fig. 6. Figure 6(a) shows a typical pulse produced by the conventional mode laser oscillator. This pulse consists of a statistical distribution (in both time and space) of normal mode transients. Each transient resembles a Gaussian pulse with a duration of 20-100 nsec. With the voltage waveform of Fig. 6(b)

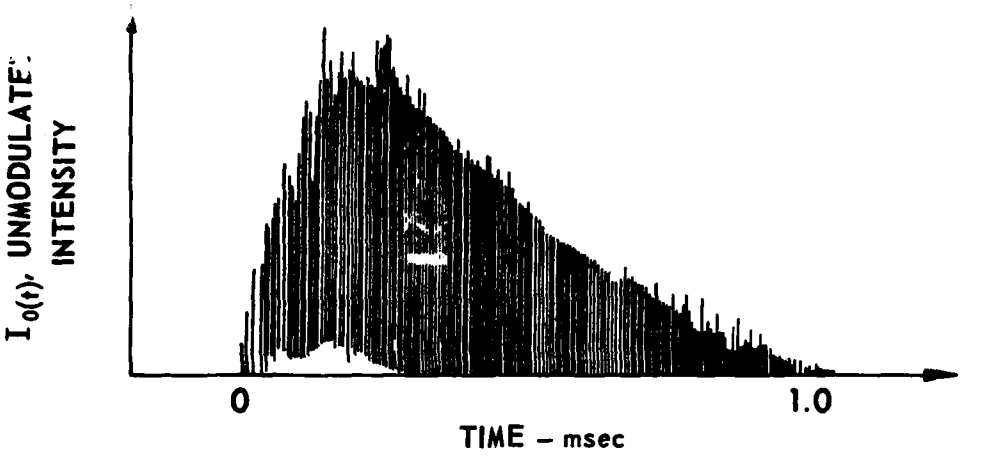

(a) NORMAL MODE LASER PULSE

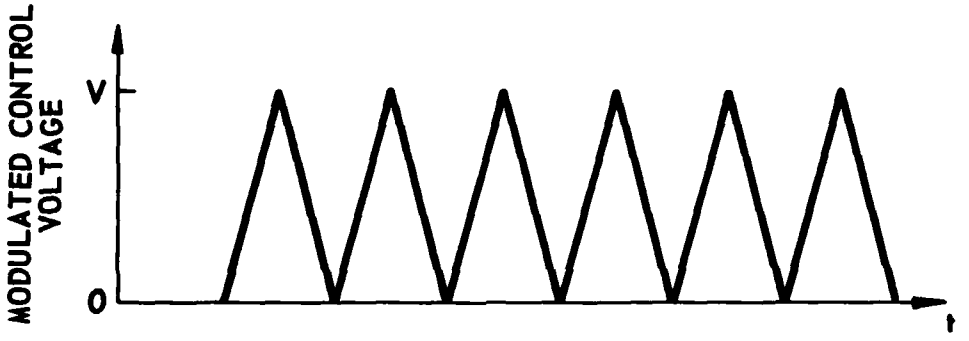

(b) MODULATION CONTROL SIGNAL

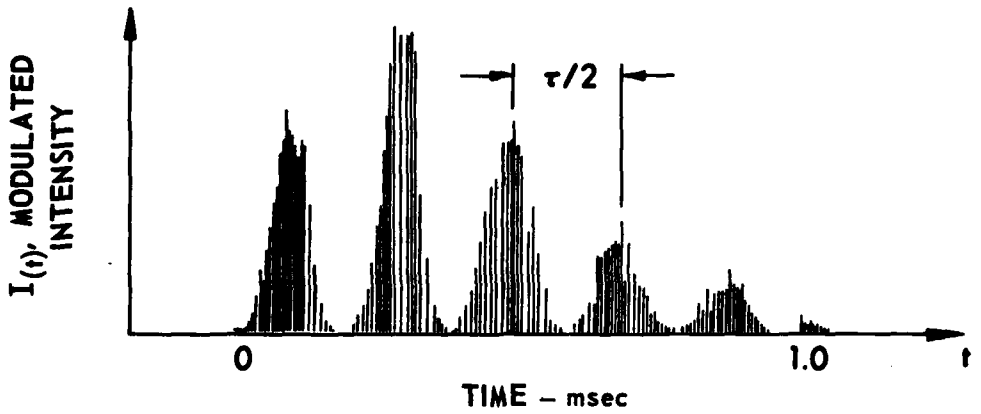

(c) MODULATED NORMAL MODE LASER PULSE

FIGURE 6
REPRESENTATIVE OPERATION OF MODULATED LASER SYSTEM

ARL - UT
AS-73-220
TGM - DR
3 - 19 - 73
REV 4-7-75

applied to the Pockels cell, the system output is the modulated laser pulse shown in Fig. 6(c). Typical peak values of modulation control voltage are 7.0 kV for the Nd:glass laser and 4.5 kV for the ruby laser.

By referring again to Fig. 4, it may be noted that the final component on the laser optical rail is the photodetector assembly. This assembly houses a beam splitter and photodiode. The voltage output of the photodiode is proportional to the intensity of the laser beam, and the integrated photodiode voltage is proportional to the total energy output of the modulated laser pulse. The photodetector is calibrated by comparing the integrated photodiode voltage to the energy measured by a Quantronix 501/504 calorimeter for the same laser pulse.

Specifications of the modulated laser system are shown in Table I. Typically the laser will produce 5 kW of modulated power in a 1 msec burst over a frequency range of 5-80 kHz. The system has a maximum repetition rate of four pulses per minute, due to the time required to charge the power supply capacitors and to the cooling requirements of the laser oscillator head.

A description of tests and maintenance that were required to make the laser system operational is given in Section III.

B. Mechanical Hardware

The experiments will be conducted in the 18.29 x 4.57 x 3.66 m (60 ft x 15 ft x 12 ft) water tank in the ARL:UT tankroom where humidity and air quality control, which are crucial to the maintenance of laser optics, can be maintained. Another consideration in designing the experimental setup is eye safety. The experimental area is surrounded by an opaque curtain; if necessary, persons inside the curtained area will wear goggles, to eliminate danger of eye damage.

TABLE I
MODULATED LASER SYSTEM SPECIFICATIONS

	OPTICAL WAVELENGTH (μ)	UNMODULATED OUTPUT energy/power	MODULATED OUTPUT energy/power	PULSE LENGTH (msec)	MODULATION FREQUENCY (kHz)	BEAM DIVERGENCE (mrad)
RUBY	0.6943	25 J 25 kW	5 J 5 kW	1.0	5 to 80	1.7
Nd:GLASS	1.06	30 J 30 kW	5 J 5 kW	1.0	5 to 80	2.2

Plans for the mechanical hardware used in the experimental system are shown in Figs. 7 and 8. The laser is mounted on a table placed near the open water of the tank. Shock mounts are used to prevent generation of acoustic signals by the mechanical shock of the laser flashtube that occurs during optical pumping of the laser rod. The table and associated mounting hardware are sufficiently rigid that the alignment of the optical hardware can be maintained.

The laser beam is deflected by a 90^{o} prism using total internal reflection, so that no reflection coatings are required. The beam passes through a tube to a rotating mirror and is deflected to the water. The total light path is about 7.62 m (25 ft) long. The reasons for having a tube in the light path are: (1) it restricts the path of the beam and thus reduces danger of eye damage, (2) it provides a rigid support between the deflection prism and the mirror mounting, and (3) sighting inside the tube can simplify beam alignment.

C. Rotating Mirror

The rotating mirror has been designed to meet the following requirements: (1) each mirror facet must be large enough to accept all of the laser beam during a laser pulse, (2) any coating on the mirror must be capable of handling the high energy densities of the incident laser beam, (3) the reflectivity of the mirror surface must be sufficiently high that severe losses in acoustic source levels are not experienced due to optical transmission loss, and (4) the mirror must be capable of rotation speeds that provide rectilinear movement of the thermoacoustic source at speeds up to Mach 2.

A detailed set of specifications to meet the above requirements was submitted to the Lincoln Laser Company in Phoenix, Arizona, and a system has been procured that meets the design requirements. A summary of the specifications of the rotating mirror system is given in Table II.

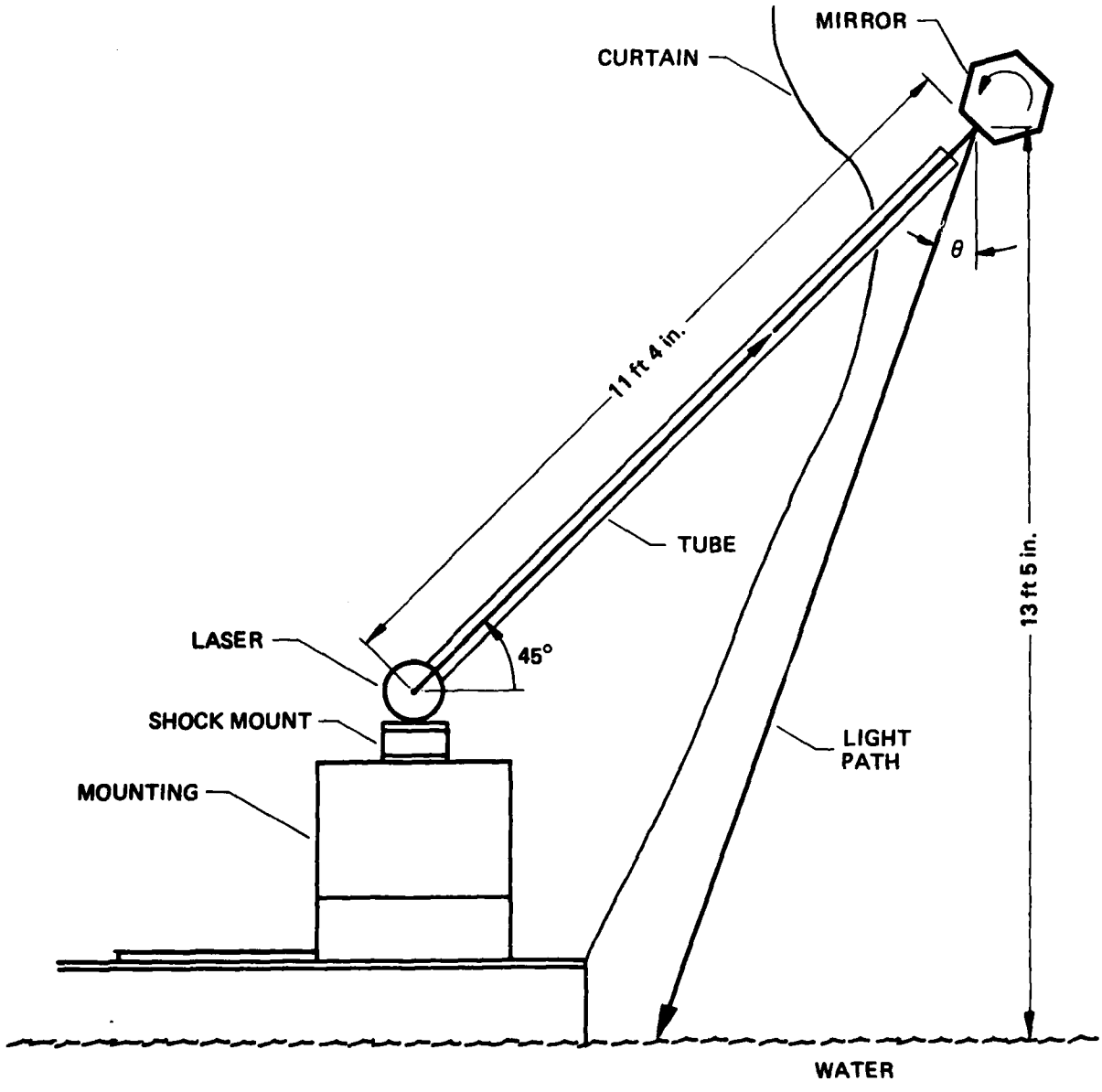

FIGURE 7
MECHANICAL ARRANGEMENT – I

ARL:UT
AS-82-1278
YHB-GA
8-12-82
REV 6-28-83

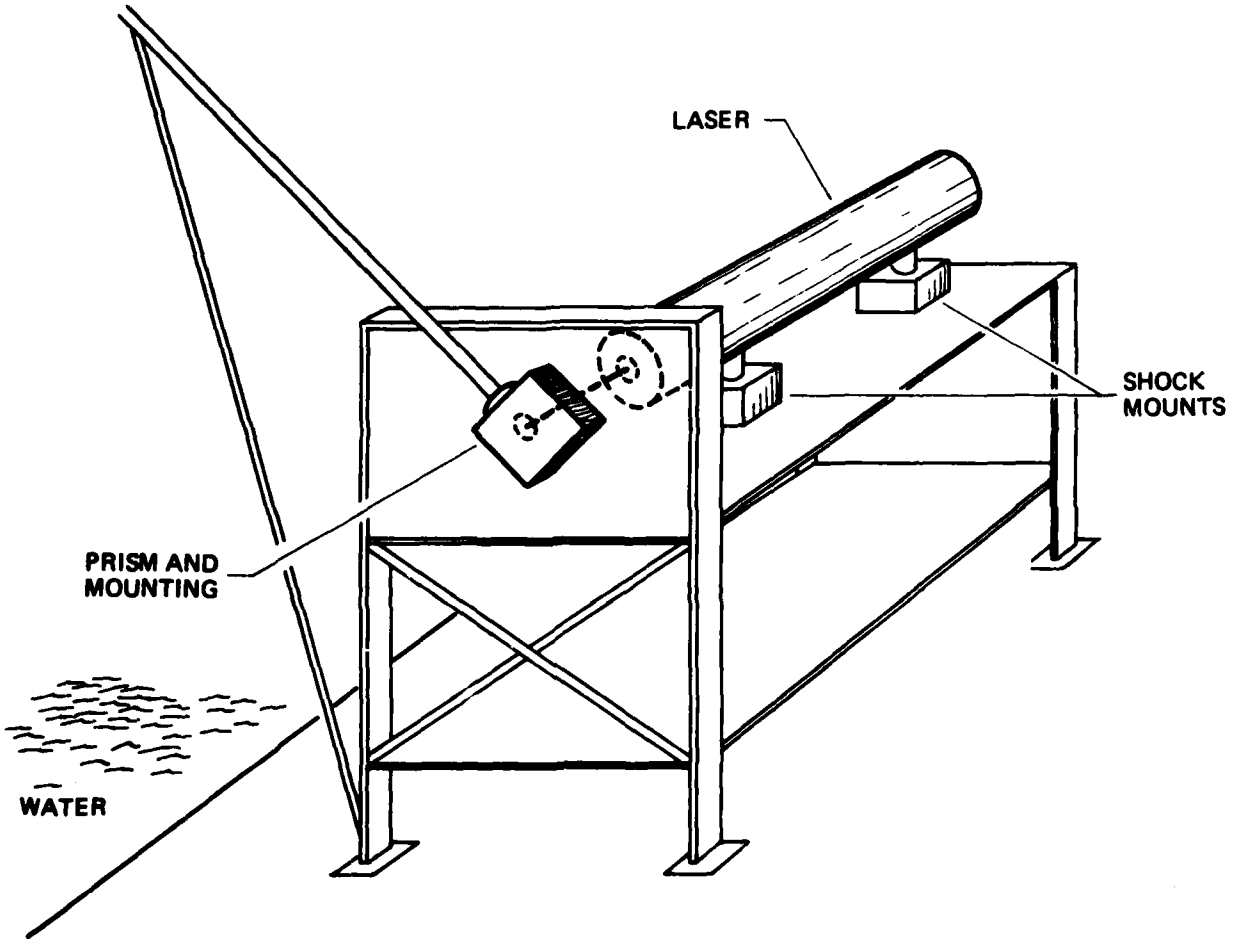

FIGURE 8
MECHANICAL ARRANGEMENT – II

ARL:UT
AS-82-1279
YHB·GA
8·12·82
REV 6-28-83

TABLE II

SPECIFICATIONS FOR THE ROTATING MIRROR SYSTEM

Mirror substrate material:	Aluminum and Thorium Flouride
Number of facets:	6
Circumscribed circle diameter:	15.2 cm (6 in.)
Facet width:	3.2 cm (1.25 in.)
Facet length:	7.6 cm (3 in.)
Surface flatness:	$\lambda/4$
Surface reflectivity:	82% at 0.6943 m 88% at 1.06 m
Speed of rotation:	150 - 3500 rpm $\pm$0.1%
Linear source speed:	$\approx$Mach 0.1 to Mach 2

D. Beam Synchronization

The experimental system must be designed so that the position of the rotating mirror and the firing of the laser are synchronized. Synchronization ensures that the thermoacoustic source moves through a known and repeatable path in the water.

One means of obtaining synchronization between laser beam and mirror uses a "reflective transducer" which consists of a light emitting diode (LED) and a phototransistor. If the light from the LED is reflected from the rotating mirror to the phototransistor, an electrical pulse will occur at the output of the phototransistor as each facet passes by the transducer. These pulses can be delayed in time and used to trigger the firing of the laser.

A reflective transducer has been procured from TRW, Inc., Carrollton, Texas, and will be used in the development of the synchronization hardware.

E. Signal Processing Hardware

The data acquisition system should have at least two channels, one for acoustic data and one for optical data. The system should be capable of measuring, storing, and analyzing transient signals.

After consideration of various digital oscilloscopes that are commercially available, the Nicolet Model 4094 oscilloscope was selected as the best choice for the experimental system. The Nicolet 4094 provides two channels with simultaneous 12-bit digitizers that sample at a rate of 2 MHz. There is provision for storage of the digitized data on a double-sided 5 1/4 in. floppy diskette. It is possible to perform mathematical operations on stored data by loading programs into the oscilloscope from diskettes. For example, integration in the time domain over specified limits can be performed and the output displayed on the oscilloscope. Additional data manipulation can be performed by loading stored data to an off-line computer via the IEEE-488 interface that is available for the oscilloscope.

The preliminary design of an automated data acquisition system is also in progress. The addition of a microcomputer with appropriate software to the experimental system would permit rapid calculation and control of the rotating mirror speed for given thermoacoustic source speeds. An automated data acquisition system would provide fast turnaround time on data analysis by calculating theoretical and experimental source levels and directivity functions. The system could also be used for database management and for storing experimental parameters and calculated results in files with the raw data.

III. PRELIMINARY TESTS AND PREDICTIONS

Concurrent with the design of the experimental system some tests were made on components of the modulated laser system and the ambient acoustic noise was measured over the frequency range of interest. The test results identified laser components whose performance has deteriorated or failed during storage since completion of work on Contract N00014-70-A-0166. The ambient noise measurement provided data necessary for predicting the signal-to-noise ratio (S/N) that could be obtained for the experiments.

A. Laser Tests

1. Output Energy

The energy of the unmodulated laser beam was measured as a function of capacitor voltage for both ruby and Nd:glass rods. The energy measurements were made by directing the laser beam into a Quantronix 504A energy meter. The measurements showed that the energy per kilovolt produced by the laser had decreased during storage, and that the maximum energy for the ruby and Nd:glass rods has decreased by 2.5 J and 5 J, respectively, from the values given in Table I. It is suspected that the loss of energy is due to deterioration of the laser flashtube. A replacement flashtube has been obtained and the tests will be repeated.

2. Laser Beam Modulation System

Both the waveform generator and the high voltage driving amplifier failed during tests. It was determined that principal cause of the failure was related to deterioration of the 10 kV vacuum tube in the output stage of the driving amplifier. A replacement tube has been obtained and repair of the modulation system continues.

3. Beam Divergence and Spot Size

The spot size of the laser beam has been determined by burning the emulsion of exposed photographic film. Measuring spot size for various ranges permits calculation of the beam divergence.

The half angle of divergence for the ruby rod was found to be 1.6 mrad, which is in good agreement with the value shown in Table I. The spot size at the output of the laser was found to be 13 mm for ruby and 20 mm for glass. Using the measured angle of divergence, the maximum spot on the rotating mirror will be an ellipse having dimensions of 30 x 25 mm for ruby and 35 x 42 mm for glass. The spot size at the water surface will be approximately a circle of 40 mm diam for ruby and 55 mm for glass.

These results are summarized in Table III.

TABLE III
SPOT SIZES

Position	Ruby Laser (θ_d=1.7 mrad)	Glass Laser (θ_d=2.2 mrad)
exit window	13 x 13 mm	20 x 20 mm
mirror	30 x 25 mm	42 x 35 mm
water	43 x 40 mm	59 x 55 mm

It should be noted that the spot size has a significant effect upon the source level of a thermoacoustic array, because of acoustic diffraction. The loss in source level for a Gaussian laser beam of finite cross-sectional area is given by[2,4]

$$\Delta L_s = 20 \log\left[\exp\left(-\frac{1}{4} k^2 a^2 \sin^2\theta\right)\right] \quad , \qquad (3)$$

where

ΔL_s is the loss due to acoustic diffraction,
a = laser beam radius,
k = acoustic wave number, and
θ is the angle from the laser beam axis to the observation point.

A simple way to reduce the loss in source level due to diffraction is to stop the laser beam with an iris, at the expense of reducing the optical power delivered to the medium. A tradeoff analysis is being conducted that will lead to decisions on spot size at the mirror, thus affecting size of each mirror facet, and on spot size at the water that will affect the source level and S/N for the experiments.

B. Acoustic Measurements and Predictions

1. Nearfield Limits

The transition from nearfield to farfield radiation regimes for a thermoacoustic array occurs at the range given by[4]

$$R_{ota} = 3k/\alpha^2 \quad , \tag{4}$$

where

k is the acoustic wave number, and
α is the optical attenuation coefficient.

Values of R_{ota} for the ruby and Nd:glass rods for selected frequencies are given in Table IV.

TABLE IV
NEARFIELD LIMITS

f (kHz)	R_{ota} (m)	
	Ruby	Nd:glass
10	56	0.57
20	112	1.2
50	280	3
80	448	5

For an array and a directional receiver combination the effective Rayleigh distance R_o can be approximated by the sum of the Rayleigh distances of the two components. In this case,

$$R_o = R_{ota} + R_{oh} \quad , \tag{5}$$

where R_{oh} = Rayleigh distance of the hydrophone.

For a piston-type receiving transducer, the Rayleigh distance is given by

$$R_{oh} = \frac{D_H^2}{\lambda} \quad , \tag{6}$$

where

D_H = diameter of transducer
λ = wavelength.

Using values of R_{oh} of the hydrophone (H23) and the more directional line-in-cone hydrophone (LC), the effective Rayleigh distance for all the thermoacoustic array/hydrophone combinations were estimated, as shown in Table V.

TABLE V
EFFECTIVE RAYLEIGH DISTANCE

f (kHz)	R_o (m)			
	Ruby		Nd:glass	
	LC	H23	LC	H23
10	65	64	1.8	0.6
20	130	128	3.6	1.2
50	325	320	9.0	3.0
80	520	512	14.3	5.0

It can be seen from the table that farfield measurements can be made in the ARL:UT tankroom for the Nd:glass rod only, unless an additional medium of high optical absorption is introduced in the path of the laser beam. For example, a rubber container filled with copper sulfate could be immersed in the water in the beam path, and the thermoacoustic signals would be coupled into the water.

2. Signal-to-Noise Ratio

The ambient noise level (NL) in the ARL:UT tankroom was measured with an H23 hydrophone over the frequency range 10-80 kHz. Average isotropic values of NL for selected frequencies are shown in Table VI. Also shown in the table are values of theoretical source levels that would be obtained from a stationary thermoacoustic array,

TABLE VI

ACOUSTIC PARAMETERS FOR SIGNAL LEVEL CALCULATIONS

f (kHz)	L_s (dB) re 1 μPa at 1 m	NL (dB) re 1 μPa 1 Hz band	DI_{LC} (dB)	DI_{H23} (dB)	L_{fb}^* Ruby	L_{fb}^* Nd:Glass
10	97.3	54	18.5	0.0	1.5	2.7
20	103.3	45	25.0	1.2	5.7	9.0
50	111.3	47	32.0	5.2	17.8	22.7
80	115.4	47	36.5	7.3	25.5	30.5

*Gaussian spot size w = 2.7 cm for the Nd:glass laser, 2.0 cm for the ruby laser; a = 2.5/k

assuming a power of 500 W entering the water. For a narrow laser beam, source level is given by[4]

$$L_s = 20 \log \frac{f\beta P_o}{4c_p} \quad , \tag{7}$$

where

f = modulation frequency in Hz,

β = coefficient of thermal expansion,

c_p = specific heat per unit mass, and

P_o = laser power in W.

The S/N is a maximum at the Rayleigh distance, and for a matched filter it is given by

$$S/N = L_s + 10 \log T - NL + DI - 20 \log R_o + 20 \log D_f - L_{fb} \quad , \tag{8}$$

where T is the pulse length, DI is the directivity index in decibels of the receiving hydrophone, D_f is the normalized directivity function of an exponentially tapered array given by

$$D_f = \frac{\alpha}{\alpha^2 + k^2 \cos^2\theta} \quad , \tag{9}$$

and L_{fb} is the loss due to finite beamwidth of the laser, given by[4]

$$L_{fb} = -20 \log \left[\frac{2}{w^2} \int_0^a J_0(kx \sin\theta) \exp\left(-\frac{x^2}{w^2}\right) x dx \right] \quad , \tag{10}$$

where θ is the declination angle of the hydrophone position with respect to the vertical array. The signal is a maximum in the broadside direction, where $\theta = \pi/2$.

It is assumed in Eq. (10) that the laser beam profile is Gaussian shaded with a 1/e radius of w, and then further limited by a circular iris aperture such that the radius of the light beam entering the water is limited to a.

We shall consider the maximum S/N in the broadside direction where the value of the directivity function D_f is unity. The values of L_{fb} were calculated using a computer program, and the results are shown in Table VI. The directivity indices DI of the hydrophones were calculated and are also shown in Table VI.

Finally, using Eq. (8), the values in Table VI and the values of R_o from Table V, the maximum S/N for each case was calculated, as shown in Table VII.

TABLE VII

MAXIMUM S/N AT R_o

f (kHz)	S/N (dB)			
	Ruby		Nd:glass	
	LC	H23	LC	H23
10	-11	-30	20	11
20	0	-24	28	13
50	-6	-27	10	13
80	0	-21	16	-3

It can be seen that adequate values of S/N ($\geq$10 dB) are predicted for the Nd:glass laser and the line-in-cone hydrophone for the total range of frequencies, and for frequencies up to 50 kHz with the H23 hydrophone. From Table V, it can also be seen that the Rayleigh distance is reasonably short, at least up to 50 kHz; with regard to both S/N and Rayleigh distance, the acoustic signals from the ruby laser are going to be more difficult to measure.

IV. SUMMARY AND CONCLUSIONS

An experimental system is being developed for studying the properties of moving thermoacoustic sources. A laser system with ruby and Nd:glass rods is used to generate the thermoacoustic source. The laser was procured under an earlier ONR contract (N00014-70-A-0166, Task 15), and is being refurbished for the current study. The laser uses a Pockels cell to provide pulsed, modulated signals over a modulation frequency range of 5-80 kHz. The laser beam is scanned over a portion of the water surface by means of a rotating mirror, which provides scanning speeds up to Mach 2. The position of the rotating mirror and the firing of the laser are synchronized so that the thermoacoustic source moves through a known and repeatable path in the water. A Nicolet Model 4094 oscilloscope has been procured to aid in the measurement, storage, and analyzing of transient acoustic signals produced by the thermoacoustic source.

Tests conducted on the laser system revealed a number of problems that needed to be resolved prior to operation of the system. Replacement parts have been procured. The laser beam spot size has been measured and it has been determined that some means of reducing the spot size at the water surface is required to minimize loss in acoustic source level due to diffraction effects.

Predictions for the effective nearfield limit of the thermoacoustic source have been made for the ruby and Nd:glass lasers over a frequency range of 10-80 kHz. It was found that the nearfield limit exceeds the dimensions of the water tank for the ruby laser, but that farfield measurements in the tank were possible for the Nd:glass laser.

Measurements of the ambient acoustic noise level in the ARL:UT tank were made over the frequency range of interest, and predictions were

made of S/N for the experimental thermoacoustic source. It was found that adequate S/N values could be obtained for the Nd:glass laser using an omnidirectional type H23 hydrophone, but the S/N values predicted for the ruby laser require the use of a line-in-cone hydrophone to provide directional reception of the thermoacoustic signals.

Further development of the experimental system and a description of the experimental results will be presented in a later report.

REFERENCES

1. P. J. Westervelt and R. S. Larson, "Laser-Excited Broadside Array," J. Acoust. Soc. Am. 54, 121-122 (1973).

2. R. S. Larson, "Laser-Excited Broadside Array Generated from a Spherically Spreading Laser Beam," J. Acoust. Soc. Am. 58, 1009-1012 (1975).

3. T. G. Muir, C. R. Culbertson, and J. R. Clynch, "Experiments on Thermoacoustic Arrays with Laser Excitation," J. Acoust. Soc. Am. 59, 735-742 (1976).

4. C. R. Culbertson, "Experimental Investigation of the Laser-Excited Thermoacoustic Array in Water," M. S. Thesis, The University of Texas at Austin, 1975, and Applied Research Laboratories Technical Report No. 75-51 (ARL-TR-75-51), Applied Research Laboratories, The University of Texas at Austin (1975).

5. L. M. Lyamshev and L. V. Sedov, "Optical Generation of Sound in a Liquid: Thermal Mechanism (Review), Sov. Phys.-Acoust. 27, 4-18 (1981).

6. F. V. Bunkin, A. I. Malyarovskii, V. G. Mikhalevich, and F. P. Shipulo, "Experimental Investigation of the Acoustic Field of a Moving Optoacoustic Antenna," Sov. J. Quantum Electron. 8, 270-271 (1978).

7. I. B. Esipov, "Radiation of Sound from a Supersonic Heat Source," Sov. Phys.-Acoust. 23, 92-93 (1977).

8. A. I. Bozhkov, F. V. Bunkin, I. B. Esipov, A. I. Malyarovskii, and M. G. Mikhalevich, "Moving Laser Thermooptical Sources of Ultra-Sound," Sov. Phys.-Acoust. 26, 100-104 (1980).

9. A. I. Bozhkov and A. A. Kolomenskii, "Acoustic Field of an Optoacoustic Antenna Moving at Subsonic or Supersonic Speed," Sov. J. Quantum Electron. 8, 1449-1454 (1978).

10. F. V. Bunkin, A. I. Malyarovskii, and V. G. Mikhalevich, "Experimental Study of Pulsed Sound Fields by Moving Laser Thermooptical Sources," Sov. Phys.-Acoust. 27, 98-102 (1981).

11. E. E. Mikeska and C. M. McKinney, "Relationship of Transducer Apertures and Separation Distances to the Directivity Patterns in the Nearfield Region," J. Acoust. Soc. Am. 56, 121-122 (1973).

15 July 1983

DISTRIBUTION LIST FOR
ARL-TR-83-24
UNDER CONTRACT N00014-82-K-0425

Copy No.	
	Office of Naval Research Department of the Navy Arlington, VA 22217
1	Attn: P. Rogers
	Director Naval Research Laboratory 455 Overlook Ave., S.W. Washington, DC 20375
2	Attn: Code 2627
3 - 14	Commanding Officer and Director Defense Technical Information Center Bldg. 5, Cameron Station Alexandria, VA 22314
	School of Mechanical Engineering Georgia Institute of Technology Atlanta, GA 30332
15	Attn: A. Pierce
	Naval Surface Weapons Center White Oak Laboratory Silver Spring, MD 20910
16	Attn: C. Bell
	Mechanical Engineering Department The University of Texas at Austin Austin, TX 78712
17	Attn: I. Bush-Vishniac
18	Advanced Sonar Division, ARL:UT
19	A. Stroup, ARL:UT
20	Yves H. Berthelot, ARL:UT
21	Nicholas P. Chotiros, ARL:UT
22	C. Robert Culbertson, ARL:UT

Distribution List for ARL-TR-83-24 under Contract N0014-82-K-0425 (Cont'd)

Copy No.

23	L. Steinborn, ARL:UT
24	Reuben H. Wallace, ARL:UT
25	Library, ARL:UT

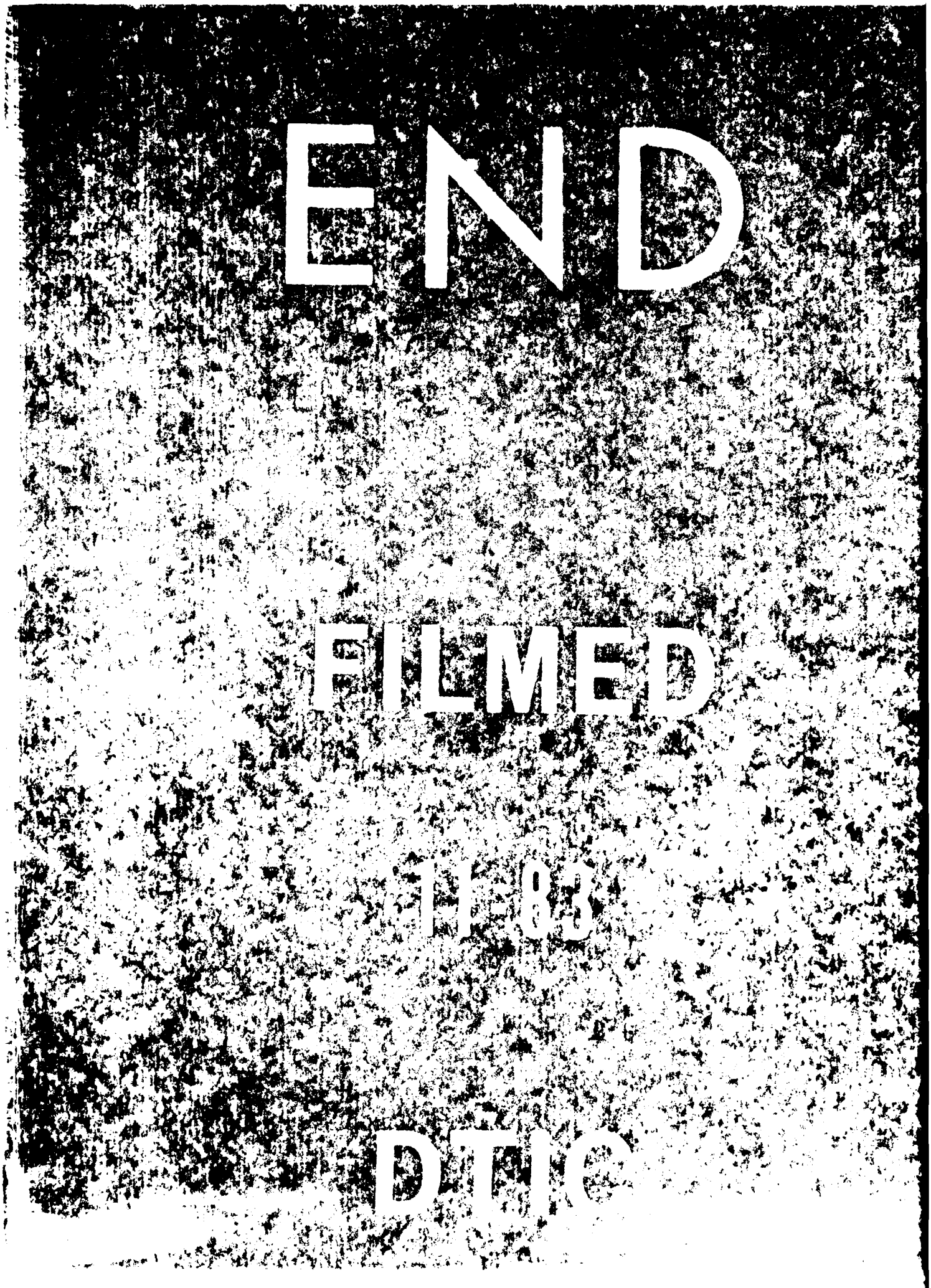
END
FILMED
DTIC